Cross sections and recoil properties of ^{83,84,86}Rb formed by 0.6–21 GeV ^{1}H reactions with targets of Y to U

M. Lagarde-Simonoff and G. N. Simonoff

Centre d'Etudes Nucléaires de Bordeaux-Gradignan, Laboratoire de Chimie Nucléaire, E.R.A. n° 144, Le Haut Vigneau-33170-Gradignan, France

(Received 15 December 1978)

Cross sections for the formation of rubidium isotopes 83, 84, and 86 have been determined for targets from yttrium to uranium irradiated by protons of 0.6, 10.5, and 21 GeV. The recoil technique, using thick targets and thick collectors, combined with a mathematical formalism based on the two step model, permits the determination of some characteristics of the nuclear reactions, i.e., the range R, the mean momentum $\langle P \rangle$ of the observed products, and the excitation energy E^* of the residual nucleus after cascade. For the three Rb isotopes at 0.6 GeV, the mean momenta fall into three groups depending on the nature of the targets: (a) less than 30 (MeV u)$^{1/2}$ for Y, Nb, and Ag but proportional to ΔA, the difference between the target and product masses, (b) about 40 to 55 (MeV u)$^{1/2}$ for the rare earths, and (c) from 55 to 120 (MeV u)$^{1/2}$ for Ta to U. For 0.6, 10.5, and 21 GeV protons, the mean momenta are all practically the same as for the first two groups of targets. On the contrary, for ^{83}Rb and ^{84}Rb formed in targets Ta to U, the momenta decrease decidedly between 0.6 and 10.5 GeV. The mean momentum of ^{86}Rb formed in Th and U seems almost the same at 10.5 and 0.6 GeV. The excitation energies E^* are very similar for 0.6, 10.5, and 21 GeV protons for all nuclear reactions where the mean momentum depends only slightly on E_p. However, the apparent value of E^* diminishes for targets showing a decrease of mean momentum at 10.5 and 21 GeV. A semi-empirical test, based on the mean squared momentum $\langle m_i^2 v_i^2 \rangle$ per evaporated nucleon, allows the production of Rb from Y, Nb, and Ag to be interpreted as spallation. Comparison of the experimental momenta or kinetic energies $\langle T \rangle$ with values $\bar{E}$ calculated from the liquid drop model suggests binary fission at medium energies for the production of all three isotopes from targets of Ta to U with 0.6 GeV protons. The same conclusion is reached for the production of ^{86}Rb from Th and U for all incident energies employed. Reactions showing anomalous behavior of E^* not explicable by the fission or simple spallation could result from a high energy mechanism.

[NUCLEAR REACTIONS ^{83}Rb, ^{84}Rb, ^{86}Rb in 13 targets (Y to U), 0.6–10.5–21 GeV E_p. Measured cross sections σ and thick target-thick collectors recoil properties. Derived deposition energy E^*, kinetic energy T and momentum per emitted nucleon.]

I. INTRODUCTION

The general influence of incident energy on the reaction products is now well known for proton-induced reactions, thanks to various techniques (radiochemistry, track detectors, etc). When projectile energies reach several GeV for uranium or tantalum targets, a strong increase of the production of neutron-deficient isotopes is observed (for products with mass of about one-half that of the target). In addition, a decrease of $\approx\frac{1}{2}$ has been observed for the ranges of these isotopes when the incident energy is raised from ≈0.6 to 6 GeV. In spite of the large amount of work carried out, a unified picture of the observed results is only now beginning to emerge.[1]

Targets of Au and U have been extensively employed, and a large body of results is available concerning cross sections[2-13] and recoil properties.[1,3,10,12-17]

For uranium targets the formation of these products, up to incident energies of about 0.5 GeV, is consistent with a binary fission mechanism.[4,18-21] With protons of several GeV, the charge dispersion curves become complex. They shift progressively with increasing energy from a fairly symmetrical Gaussian centered on the neutron-excess isotopes at 0.5 GeV to a form with two peaks situated on either side of stability. Such behavior has been observed for $A \approx 109$ (Ref. 22), $A = 111$ (Ref. 15), $A = 117$ (Ref. 23), $A \approx 130$ (Refs. 2, 4), $A = 131$ (Ref. 12), and $A \approx 147$ (Ref. 11). The isotope distributions obtained for elements such as antimony,[6] iodine,[5,14] xenon,[13] and cesium,[7] show a marked increase in the production of neutron-deficient isotopes with an increase of incident energy. The same result is also observed with lighter elements such as bromine[14] and rubidium.[7] Experiments using the thick-target, thick-catcher recoil technique show that the ranges of the neutron-deficient isotopes are comparable with those of the neutron-excess isotopes at 0.5 GeV, but fall by about one-half

for protons of several GeV. In contrast, the ranges of the excess-neutron isotopes fall by only a few percent over a similar energy span. Examination of the relative production rates and ranges for different isobars shows that the transition from longer to shorter ranges takes place over an interval of two units of Z. In the case of bromine isotopes, the reduction of the range takes place over two or three units of A. The ranges begin to fall at the stability line (approximately the minimum between the two peaks of the charge-dispersion curves) and continue to fall for the neutron-deficient isotopes. Comparison of isotope distributions of iodine formed in uranium targets with those formed in lighter targets (rare earths, tantalum, and gold) induced Rudstam and Sørensen[5] to propose two mechanisms, fission for the excess-neutron products and spallation for the neutron-deficient. Beg and Porile[10] suggested that fragmentation (an intranuclear cascade with ejection of fragments in the forward direction, followed by a long evaporation chain) can account for the lower ranges of the neutron-deficient products of barium and strontium. This fast process had been suggested by Alexander, Baltzinger, and Gazdik[3] for neutron-deficient iodine isotopes produced with 6.2 GeV protons from uranium. An analysis that established a correlation between the observed range of an element and its position on the charge-dispersion curve led Starzyk and Sugarman[17] to propose three processes for the formation of isobars of mass $A = 111$: namely, spallation in which preferential forward emission of fragments could take place during the cascade, and two fission processes, with high and low energy deposition. Clearly, the production of neutron-deficient products in uranium targets is complex.

With lighter targets, it is found that the behavior of products ($100 < A < 113$) formed in lead targets[24] is entirely analogous to that observed with uranium, both with regard to charge dispersion and range.

The dependence of recoil properties on incident energy and mass number of product has been extensively studied for reactions of protons with gold.[1] The mean momenta of the recoiling nuclei at 1 GeV incident energy indicate a substantial fission contribution to the formation of products in the mass range $A = 46$–103. At higher bombarding energies, the momenta of the neutron-deficient products in this mass range decreases, showing that the deep spallation is becoming more prominent. The momenta of neutron-excess nuclides decreases by a smaller amount or not at all, depending on the proportions of fission and deep spallation.

With a tantalum target, the isotope distribution of rubidium is perfectly Gaussian[7] for energies of several GeV, and so is the charge distribution of the isobaric chain $A = 86$.[25] The ranges of the neutron-deficient isotopes are no more than about half their values at 1 GeV, but this reduction occurs also for the neutron-excess isotopes.[26]

Faced with the complex and fragmentary pattern formed by all these results, we felt that a study of the properties of some neutron-deficient and neutron-excess products from various targets should yield an interesting contribution to our understanding of nuclear reactions at high energies. We have therefore determined the cross sections and the recoil properties of ^{83}Rb, ^{84}Rb, and ^{86}Rb, formed in 13 targets ranging from yttrium to uranium, using protons of 0.6, 10.5, and 21 GeV. Extensive tests have been made for spallation from targets of mass close to those of the observed products. With regard to fission, the kinetic energies of the fragments have been compared with those calculated according to Nix and Swiatecki.[27,28] In this way, a number of results have been interpreted as primarely due to spallation or fission. Those processes not well explained by fission or spallation can be accounted for by means of a cascade process which includes the ejection of fragments.

II. EXPERIMENTAL METHODS

A. Targets

The experiments carried out in this work required two types of target stacks, depending on whether cross sections or recoil properties (Fig. 1) were to be studied. In the first case, targets, monitors, and aluminum guards of the same dimensions were rigorously aligned. For the determination of recoil properties, the thick-target, thick-collector technique was employed. Each target was enclosed in aluminum foil, to collect the recoil ions in the forward or backward directions. A blank foil was placed between each assemblage to determine the amount of parasitic activity created by reactions of the protons with the impurities in the aluminum (<1% of the total activity of the recoils). The dimensions of the collectors and the

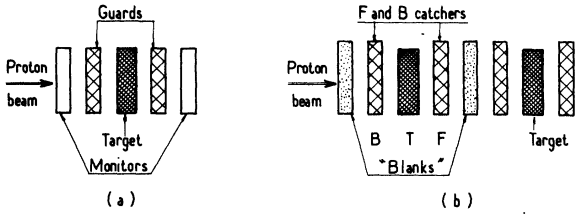

FIG. 1. The target assembly for cross section (a) and forward-backward (b) experiments.

blanks were slightly larger than those of the targets and extended about 0.2 cm beyond the edge of the latter. In all experiments, the aluminum used for collectors, guards and monitors was of 99.999% purity and 0.0050 cm thick. The isotopic composition of the target elements corresponded to the natural distribution. Depending on the material, the purity varied from 99.5% to 99.999% and the thickness from 9 to 200 mg/cm^2, as shown in Table I.

The influence of secondary particles was examined by varying the thickness of the targets, particularly in the case of uranium. The oxide films on targets of U and Th were removed by 6N HNO_3 and organic matter was eliminated with various solvents. The separate parts of the assemblage were then dried, weighed, and stacked in the appropriate fashion.

B. Irradiations

Irradiations by 0.6 GeV protons were made using the internal beam of the synchrocyclotron (SC) at CERN. The target holder consisted of two aluminum jaws clamping a rectangular stack of targets of 2.0 cm×1.8 cm and of aluminum foils of 2.2 cm ×2.0 cm for the recoil experiments. The stack extended about 0.6 cm beyond the edge of the target holder.

Irradiations by protons of 10.5 and 21 GeV were carried out with the protonsynchrotron (PS) at CERN, using the internal beam in most cases. With the internal beam, the target holder was approximately semicircular and a half-circle of the stack (about 3 cm diam) was exposed to the beam. Studies of the dispersion of the beam have shown it to be circular in cross section, with a diameter of about 2 cm. For reasons of precision, a triangular fraction of the irradiated stack, representing on the average 85% of the total activity, is taken for subsequent measurements. With the external beam, the stacks were simpler. Targets and aluminum collectors were of the same dimensions and were held by a square target holder (2.5 cm ×2.5 cm) with a circular opening of 2.0 cm diameter.

For cross section measurements, one to two hours of irradiation with the internal beam (PS or SC) were sufficient, and the integrated flux reached 10^{16} to 10^{17} protons, on the average. For recoil experiments, the time of exposure was approximately doubled. The flux was monitored by the reaction $^{27}Al(p,3p3n)^{22}Na$: The irradiations were carried out in Geneva and all the measurements and chemical separations in Bordeaux. The values adopted for the cross section for ^{22}Na[29] were 13.5, 10.5, and 10.0 mb, for energies of 0.6, 10.5, and 21 GeV, respectively.

The formation of ^{22}Na from ^{27}Al is not very sensitive to low energy secondary particles formed by the passage of the beam through the target assemblage. The correction to the ^{22}Na activity as a function of the thickness traversed was determined experimentally and was found not to exceed 5% in the least favorable case.

TABLE I. Purity and thickness of the target materials (all had natural abundances).

Target	Purity (%)	Thickness (mg/cm^2)
Y	99.9	15
Nb	99.5	70–100
Ag	99.999	50
Pr	99.9	70–100
Tb	99.9	70–100
Ho	99.9	70–100
Tm	99.9	70–100
Ta	99.9	100
Re	99.99	70
Au	99.999	100–150
Bi	99.999	50–100
Th	99.5	100–200
U	99.7	9–200

C. Chemical separations

The rubidium isotopes were separated by classical radiochemical methods.[30] Targets, collectors, and blanks were separately dissolved by various acids (HNO_3, HCl, HF), depending on the element. After addition of weighable amounts of carrier (15 ml of a 10 mg/ml solution of natural rubidium chloride), each solution was divided into three equal volumes. The rubidium was precipitated as the perchlorate by means of concentrated HNO_3 and 70% perchloric acid at 0°C, in presence of absolute ethanol. The perchlorate was purified as follows: Metals were coprecipitated with Fe^{3+} hydroxides in 6N NH_4OH. The alkaline earths were eliminated as carbonates by 0.2 M Na_2CO_3 in the presence of barium and strontium chlorides (all of the alkaline earth metals precipitate with rubidium during the perchlorate formation). The decay periods of the isotopes of Na and Rb of interest here are such that Na does not interfere with the Rb measurements. Cesium was complexed by formation of the double iodide of cesium and bismuth, $Cs_3Bi_2I_9$, and potassium remained in solution during the selective precipitation of rubidium as the hexachlorostannate, $RbSnCl_6$. The rubidium was finally obtained as $RbClO_4$ (with a yield of 45 to 60%) on a plastic disk and covered with a Mylar film 5 μm thick.

D. Detection

Where the disintegration schemes allow (^{84}Rb, ^{86}Rb), the activity was measured by β and γ detection. A Geiger-Muller type counter with flowing methane and a low background was employed, as well as a NaI(Tl) crystal detector (7.6 cm × 8.9 cm), combined with a multichannel pulse-height analyzer. The relevant decay characteristics are shown in Table II for the isotopes studied (^{83}Rb, ^{84}Rb, ^{86}Rb). Because of the resolution of the γ detection unit, the three lines of ^{83}Rb corresponding to 0.521, 0.530, and 0.533 MeV[31] gave only a single peak. In addition, this peak also contained a contribution from the annihilation γ of the β^+ emitter, ^{84}Rb at 0.511 MeV. Using the measured activity of ^{84}Rb at 0.880 MeV, however, along with the associated branching ratio, the contribution of this isotope to the activity of ^{83}Rb could be determined.

The efficiency of the detectors for ^{86}Rb was measured by means of calibrated sources furnished by the Commissariat a l'Energie Atomique. Since neither ^{83}Rb nor ^{84}Rb was available, the efficiency, ϵ, of the γ detector for these two isotopes was obtained by interpolation from the calibrated sources of ^{85}Sr, ^{22}Na, ^{54}Mn, ^{65}Zn, ^{86}Rb, ^{24}Na, and ^{88}Y. For measurement of the β activity of ^{84}Rb, an indirect determination of the efficiency was made. The value of ϵ was obtained from the ^{84}Rb activities measured in uranium targets, using the known value[2] of σ (^{84}Rb) at 0.6 GeV [3 mb with monitoring by ^{27}Al($p,3pn$)^{24}Na, using a value of 10.5 mb for $\sigma(^{24}\mathrm{Na})$]. The various efficiencies obtained are collected in Table II. After correction for branching factors and efficiencies, the activities of the isotopes ^{84}Rb and ^{86}Rb (measured by both β and γ detection) differed by less than 3% in general. The mean of the values given by the two methods was taken.

Four activity measurements were carried out per decay period, and the measurements were repeated until the activity remained unchanged during two periods, apart from statistical fluctuations. These precautions were taken in order to subtract correctly the β contribution due to the activity of ^{87}Rb ($E_\beta = 274$ keV, $T = 4.8 \times 10^{10}$ yr) in the natural rubidium used as carrier. The decay curves were analyzed by a classical least squares method.[32] Taking into account the position of ^{83}Rb, ^{84}Rb, and ^{86}Rb in the periodic table and the delay between irradiation and chemical separations, the yield is found to be cumulative for ^{83}Rb and independent for ^{84}Rb and ^{86}Rb.

E. Precision

Two types of uncertainties must be considered, i.e., random errors and systematic errors. The first arise from measurements of the thickness of targets, inhomogeneity of monitors, and from weighing (3%), from evaluation of the chemical yield (2%), and particularly from the determination of the activities at the time of origin (1 to 10% in the case of weak activities). Systematic errors arise from the determination of the flux [$\sigma(^{22}\mathrm{Na})$ to about 10%], the determination of the efficiency of the counters employed as described and the precision of the calibrated sources (about 5%). If these various errors are added, the overall uncertainties in the absolute activities vary from 21 to 30%. This must be taken into account when comparing our cross sections with those already published elsewhere in the literature. For the recoil experiments, systematic effects are eliminated and only the random errors remain. The errors given in the tables of cross sections and recoil properties are the root mean square deviations observed for repeated experiments.

TABLE II. Radioactive properties of rubidium isotopes and efficiency factors for β and γ detection.

Isotope	$T_{1/2}$ in days	Detection	Energy (MeV)	Branching ratio (%)	Efficiency (%)
^{83}Rb	83	γ	0.521	23	
			0.530	31	8.5
			0.553	8	
^{84}Rb	33	γ	0.880	74	6.6
			0.510	42	8.5
		β	0.80 E_{β^+}	11	
			1.66 E_{β^+}	10	19
			0.91 E_{β^-}	3	
^{86}Rb	18.66	γ	1.08	8.8	5.8
		β	0.71 E_{β^-}	8.8	37.5
			1.78 E_{β^-}	91.2	

TABLE III. Cumulative ^{83}Rb and independent ^{84,86}Rb yields in mb, measured at 0.6, 10.5, and 21 GeV protons (the indicated error is the standard deviation from the mean).

E_p	Target	^{83}Rb	^{84}Rb	^{86}Rb
0.6 GeV	Y	93 ± 4 (3)	11.3 ± 1.5 (3)	3.5 (1)
	Nb	62 ± 3 (4)	4.17 ± 0.25 (4)	0.36 (1)
	Ag	14.90 ± 0.25 (4)	0.65 ± 0.02 (4)	0.10 ± 0.03 (2)
	Pr	0.15 ± 0.06 (3)	0.017 ± 0.004 (3)	0.005 ± 0.004 (2)
	Tb	0.10 ± 0.04 (9)	0.028 ± 0.008 (9)	0.010 ± 0.003 (2)
	Ho	0.10 ± 0.01 (7)	0.037 ± 0.006 (7)	0.018 ± 0.001 (7)
	Tm	0.11 ± 0.01 (7)	0.054 ± 0.007 (7)	0.017 (1)
	Ta	0.25 ± 0.02 (8)	0.12 ± 0.01 (6)	0.08 ± 0.02 (3)
	Re	0.49 ± 0.01 (5)	0.25 ± 0.02 (5)	0.16 (1)
	Au	1.42 ± 0.11 (6)	0.85 ± 0.02 (8)	0.68 ± 0.04 (4)
	Bi	2.9 ± 0.3 (5)	2.03 ± 0.07 (5)	3.11 ± 0.04 (4)
	Th	2.36 ± 0.15 (6)	2.03 ± 0.10 (6)	5.02 ± 0.02 (6)
	U	2.21 ± 0.13 (6)	2.31 ± 0.20 (5)	6.7 ± 0.1 (6)
10.5 GeV	Y	39 ± 2 (2)	10.9 ± 0.8 (2)	
	Ag	16 ± 2 (2)	2.3 ± 0.4 (2)	
	Ho	6.00 ± 0.12 (2)	0.84 ± 0.03 (2)	0.27 ± 0.01 (2)
	Ta	5.60 ± 0.54 (5)	1.14 ± 0.17 (5)	0.34 ± 0.03 (2)
	Au	6.65 ± 0.12 (2)	1.41 ± 0.05 (2)	0.57 ± 0.05 (2)
	Th	10.6 ± 1.3 (5)	5.22 ± 0.51 (5)	5.54 ± 0.06 (2)
	U	12.9 ± 1.5 (5)	6.65 ± 0.97 (5)	6.8 ± 0.3 (2)
21 GeV	Ag	19 ± 1 (3)	3.5 ± 0.4 (3)	
	Ho	8.4 ± 0.8 (9)	1.2 ± 0.5 (9)	
	Tm	9.03 ± 0.25 (3)	1.65 ± 0.15 (3)	
	Ta	8.1 ± 0.4 (4)	1.80 ± 0.05 (4)	
	Au	7.9 ± 0.9 (6)	2.3 ± 0.2 (6)	
	Th	9.2 ± 1.0 (6)	4.6 ± 0.8 (6)	
	U	12.4 ± 1.1 (2)	5.9 ± 0.1 (2)	

TABLE IV. Recoil data for ^{83}Rb: F/B, $W(F-B)$, $2W(F+B)$, η, and $\langle v \rangle$.

E_p	Target	F/B	$W(F-B)$	$2W(F+B)$	η	$\langle v \rangle$ [(MeV/u)$^{1/2}$]
0.6 GeV	Y	7.4 ± 1.6	0.12 ± 0.01	0.32 ± 0.02	0.34 ± 0.02	0.059 ± 0.005
	Nb	6.5 ± 2.1	0.22 ± 0.01	0.61 ± 0.05	0.39 ± 0.03	0.096 ± 0.012
	Ag	7.9 ± 0.6	0.49 ± 0.01	1.28 ± 0.04	0.42 ± 0.02	0.139 ± 0.010
	Tb	1.7 ± 0.1	0.37 ± 0.19	2.86 ± 0.38	0.12 ± 0.07	0.062 ± 0.040
	Ho	1.7 ± 0.3	0.45 ± 0.08	3.62 ± 0.17	0.12 ± 0.03	0.074 ± 0.021
	Ta	1.7 ± 0.1	1.01 ± 0.04	7.38 ± 0.15	0.13 ± 0.01	0.152 ± 0.011
	Re	1.5 ± 0.3	0.72 ± 0.30	7.57 ± 0.88	0.09 ± 0.01	0.111 ± 0.027
	Au	1.6 ± 0.1	0.89 ± 0.09	8.11 ± 0.25	0.11 ± 0.01	0.128 ± 0.015
	Bi	1.5 ± 0.1	0.80 ± 0.07	8.64 ± 0.38	0.09 ± 0.01	0.111 ± 0.017
	Th	1.3 ± 0.1	0.75 ± 0.08	10.62 ± 0.50	0.08 ± 0.01	0.116 ± 0.022
	U	1.3 ± 0.1	0.70 ± 0.08	10.88 ± 0.35	0.06 ± 0.01	0.092 ± 0.015
10.5 GeV	Y	2.5 ± 0.5	0.06 ± 0.01	0.29 ± 0.03	0.17 ± 0.02	0.032 ± 0.004
	Ag	2.1 ± 0.6	0.19 ± 0.01	1.07 ± 0.14	0.15 ± 0.02	0.054 ± 0.012
	Ho	1.5 ± 0.2	0.29 ± 0.02	3.13 ± 0.21	0.09 ± 0.01	0.049 ± 0.008
	Ta	1.3 ± 0.1	0.25 ± 0.02	3.96 ± 0.13	0.060 ± 0.008	0.041 ± 0.006
	Au	1.2 ± 0.1	0.20 ± 0.02	4.25 ± 0.16	0.051 ± 0.006	0.035 ± 0.004
	Th	1.1 ± 0.2	0.16 ± 0.01	5.86 ± 0.49	0.030 ± 0.004	0.026 ± 0.005
	U	1.1 ± 0.1	0.19 ± 0.02	7.28 ± 0.34	0.026 ± 0.005	0.026 ± 0.006
21 GeV	Ag	2.3 ± 0.4	0.14 ± 0.01	0.73 ± 0.05	0.16 ± 0.02	0.047 ± 0.008
	Ho	1.7 ± 0.2	0.30 ± 0.01	2.35 ± 0.12	0.11 ± 0.01	0.109 ± 0.014
	Tm	1.6 ± 0.2	0.27 ± 0.03	2.34 ± 0.16	0.10 ± 0.02	0.100 ± 0.020
	Ta	1.5 ± 0.3	0.33 ± 0.03	3.13 ± 0.33	0.09 ± 0.02	0.053 ± 0.014
	Au	1.3 ± 0.3	0.26 ± 0.09	3.66 ± 0.27	0.06 ± 0.02	0.039 ± 0.017
	Th	1.1 ± 0.2	0.17 ± 0.04	5.42 ± 0.48	0.03 ± 0.01	0.023 ± 0.009
	U	1.1 ± 0.2	0.14 ± 0.01	6.87 ± 0.77	0.020 ± 0.004	0.019 ± 0.005

III. RESULTS

A. Cross sections

Table III gives the cross sections obtained for ^{83}Rb, ^{84}Rb, and ^{86}Rb from various targets (yttrium to uranium) for protons of 0.6, 10.5, and 21 GeV. The cumulative yield of ^{83}Rb was deduced from γ activity measurements. The independent yields of ^{84}Rb and ^{86}Rb correspond to the mean values obtained from β and γ detection. The number of experiments is shown in brackets and the estimated error refers only to the reproducibility of the results obtained. For each target, the activity was corrected for losses by recoil, using the results of the recoil studies. Secondary particles of low energy do not appear to contribute to the production of rubidium. The low energy fission yields for ^{86}Rb (Refs. 33, 34) and ^{84}Rb are so small in uranium targets that no correction for this effect was necessary. This conclusion was confirmed by using targets of thickness varying from several microns to several tens of microns.

B. Recoil properties

1. Ratio F/B and experimental range, 2W(F + B)

The recoil data obtained directly from experiment are the ratio F/B and the experimental range $2W(F+B)$. F and B are the fractions collected in the forward and backward directions with respect to the total number of atoms of rubidium formed in the target. (See Tables IV and V.) W is the thickness of the target in mg/cm^2. The collected activities could have been increased by ions coming from the upper and lower edges of the targets. In view of their average thickness, it is estimated from experimental results[35] that multiplication of F and B by the factor 0.985 gives a reasonable correction for these edge effects.

Scattering effects at the target-catcher interface must also be taken into account. Particularly in the case of heavy targets, the activity fractions F and B collected in aluminum are slightly different from the values which would be obtained with a collector material closer in Z to the target. The in-

TABLE V. Recoil data for ^{84}Rb at 0.6, 10.5, 21 GeV and ^{86}Rb at 0.6, 10.5 GeV: F/B, $W(F-B)$, $2W(F+B)$, η, and $\langle v \rangle$.

E_p	Target	F/B	$W(F-B)$	$2W(F+B)$	η	$\langle v \rangle$ [(MeV/u)$^{1/2}$]
0.6 GeV	Y	4.8 ± 0.3	0.09 ± 0.01	0.28 ± 0.01	0.30 ± 0.01	0.052 ± 0.003
	Nb	10.3 ± 2.5	0.20 ± 0.01	0.50 ± 0.04	0.34 ± 0.04	0.076 ± 0.012
	Ag	7.2 ± 1.6	0.42 ± 0.01	1.12 ± 0.07	0.41 ± 0.04	0.126 ± 0.016
	Tb	1.5 ± 0.3	0.34 ± 0.27	3.30 ± 1.10	0.09 ± 0.05	0.057 ± 0.040
	Ho	1.6 ± 0.4	0.55 ± 0.22	4.55 ± 1.55	0.12 ± 0.07	0.092 ± 0.068
	Ta	1.6 ± 0.1	1.03 ± 0.05	8.96 ± 0.17	0.11 ± 0.01	0.151 ± 0.012
	Re	1.6 ± 0.1	1.09 ± 0.10	8.62 ± 0.30	0.13 ± 0.01	0.166 ± 0.025
	Au	1.3 ± 0.1	0.65 ± 0.06	9.19 ± 0.19	0.072 ± 0.008	0.097 ± 0.012
	Bi	1.3 ± 0.1	0.66 ± 0.05	8.99 ± 0.12	0.077 ± 0.006	0.099 ± 0.008
	Th	1.3 ± 0.1	0.64 ± 0.04	10.32 ± 0.25	0.061 ± 0.005	0.086 ± 0.008
	U	1.3 ± 0.1	0.61 ± 0.07	10.81 ± 0.40	0.06 ± 0.01	0.091 ± 0.015
10.5 GeV	Y	2.1 ± 0.2	0.04 ± 0.01	0.26 ± 0.01	0.13 ± 0.01	0.024 ± 0.003
	Ag	2.2 ± 0.7	0.15 ± 0.01	0.83 ± 0.11	0.16 ± 0.02	0.047 ± 0.010
	Ho	1.4 ± 0.1	0.30 ± 0.03	3.27 ± 0.09	0.08 ± 0.01	0.048 ± 0.006
	Ta	1.3 ± 0.1	0.30 ± 0.01	4.61 ± 0.07	0.060 ± 0.002	0.046 ± 0.002
	Au	1.3 ± 0.2	0.30 ± 0.02	4.67 ± 0.32	0.060 ± 0.007	0.042 ± 0.006
	Th	1.1 ± 0.1	0.17 ± 0.01	7.51 ± 0.40	0.024 ± 0.003	0.027 ± 0.005
	U	1.1 ± 0.2	0.20 ± 0.03	8.73 ± 0.75	0.022 ± 0.005	0.027 ± 0.008
21 GeV	Ag	2.4 ± 1.3	0.16 ± 0.01	0.78 ± 0.18	0.18 ± 0.05	0.053 ± 0.021
	Ho	1.7 ± 0.6	0.32 ± 0.03	2.46 ± 0.44	0.11 ± 0.03	0.111 ± 0.043
	Tm	1.8 ± 0.3	0.29 ± 0.04	2.01 ± 0.17	0.11 ± 0.03	0.089 ± 0.027
	Ta	1.6 ± 0.2	0.36 ± 0.02	3.17 ± 0.16	0.10 ± 0.01	0.057 ± 0.007
	Au	1.4 ± 0.2	0.34 ± 0.06	4.11 ± 0.37	0.07 ± 0.02	0.049 ± 0.015
	Th	1.1 ± 0.1	0.13 ± 0.06	7.63 ± 0.21	0.018 ± 0.002	0.020 ± 0.002
	U	1.1 ± 0.1	0.12 ± 0.02	9.42 ± 0.69	0.013 ± 0.003	0.016 ± 0.004
0.6 GeV	Au	1.33 ± 0.11	0.722 ± 0.083	10.100 ± 0.450	0.073 ± 0.011	0.101 ± 0.019
	Bi	1.30 ± 0.08	0.643 ± 0.091	9.978 ± 0.338	0.060 ± 0.010	0.081 ± 0.015
	Th	1.29 ± 0.11	0.629 ± 0.077	10.198 ± 0.458	0.065 ± 0.010	0.089 ± 0.017
	U	1.23 ± 0.13	0.572 ± 0.071	11.198 ± 0.610	0.050 ± 0.008	0.072 ± 0.015
10.5 GeV	Th	1.07 ± 0.10	0.261 ± 0.017	9.510 ± 0.449	0.027 ± 0.003	0.035 ± 0.005
	U	1.04 ± 0.03	0.254 ± 0.022	10.852 ± 0.153	0.023 ± 0.002	0.031 ± 0.002

creases of the quantities WF and WB have been corrected for, using experimental results[35] giving the range of fission products in the collectors aluminum and lead.

No account has been taken of factors such as nonhomogeneity of targets, Rutherford scattering of initially charged fragments and nonuniformity of the target surface.

2. *Kinetic energy, T, and mean momentum ⟨P⟩*

For the range R see the appendix. To pass from the range to the associated kinetic energy, T, requires a range-energy relation for the recoiling atom in the stopping medium.[36-38] As the following development indicates, the best choice appears to depend on the energy region involved.

The range-energy relations of Bohr, Lindhard, Scharff, and Schiøtt (LSS), and Northcliffe and Schilling give acceptable results for low energy products, provided the experimental range is corrected for multiple scattering. For high energy products, like fission fragments, on the contrary, certain authors[39-41] have noted that the kinetic energies calculated by the LSS method or obtained from tables[36] are much lower than those measured in time-of-flight experiments.[42] Thanks to the agreement between the experimental results and the Bohr relation, a corrective factor of 1.34 has been determined which may be applied to the values obtained according to Northcliffe and Schilling for rubidium in uranium. With targets of gold and tantalum, the correction factors are 1.19 and 1.13, respectively. These values were determined by comparing the experimental ranges of fission products in different media, Al, Au, Pb, and U.[35,43] If the relations of LSS are used, a better agreement for the kinetic energy of the fission products in the time-of-flight experiment is obtained when $\xi_e = Z_1^{1/6}$ is replaced by $\xi_e' = Z_1^{0.211}$.

TABLE VI. ^{83,84,86}Rb cross sections from other work. In Refs. 2 and 45, the proton flux was determined by the monitor reaction ^{27}Al(p, $3pn$)^{24}Na.

Target	E_p	Rb isotope	σ in mb	References
Ag	11.5 GeV	83	12.3 ± 0.4	55
		84	1.31 ± 0.02	
Ho	450 MeV	86	0.023 [a]	44
Ta	450 MeV	86	0.076 [a]	44
	680 MeV	86	0.120 [a]	
Re	450 MeV	86	0.37 [a]	44
Au	450 MeV	86	0.89 [a]	44
Pb	600 MeV	83	2.01 ± 0.17	64
		84	2.32 ± 0.13	
		86	3.04 ± 0.26	
Bi	450 MeV	86	4.1 [a]	44
Th	450 MeV	86	3.2 [a]	44
U	450 MeV	83	1.4 ± 0.1	2
		84	2.0 ± 0.1	
		86	6	
	600 MeV	84	3.0	2
		86	7.8	
	680 MeV	83	3.6 ± 1.2	2
		84	3.6 ± 1	
		86	8.3 ± 0.5	
	6.2 GeV	84	5.2 ± 1.1	2
		86	6.9 ± 0.4	
	28.5 GeV	84	6.88 ± 0.33	45
		86	7.27 ± 0.34	
Th	28.5 GeV	84	6.55 ± 0.37	45
		86	6.75 ± 0.37	

[a] Uncertainties larger than 30%.

The kinetic energies of the isotopes of rubidium have been determined by the three types of range-energy relations, using the appropriate corrections mentioned above. The following tables give the average value, $\langle T\rangle$, obtained, and the maximum difference is expressed between brackets as a percentage.

The mean momenta are defined as $\langle P\rangle = A\langle V\rangle$ in units of $(\text{MeV u})^{1/2}$, A being the mass of observed product. The results are presented in this way rather than directly as velocity, V, in addition to kinetic energy, $T = P^2/2A$, in order to facilitate comparison with binary fission and with the results of Kaufman, Steinberg, and Weisfield.[1]

3. *Excitation energy of the residual cascade nucleus*

A relation exists between the excitation energy, E^*, of the residual cascade nucleus and the mean velocity component of the target parallel to the beam, $\langle v_{\parallel}\rangle$, transferred by the incident proton[1]:

$$\frac{E^*}{E^*_{\text{CN}}} \approx 0.80\,\frac{\langle v_{\parallel}\rangle}{v_{\text{CN}}}\,. \qquad (1)$$

v_{CN} and E_{CN} are, respectively, the velocity and the excitation energy of a hypothetical compound nucleus formed by fusion of the proton and the target nucleus. The validity of Eq. (1) will be discussed further on.

IV. DISCUSSION OF THE RESULTS

The present results will be compared with those expected for the mechanisms of spallation and fission, which have often been used to describe nuclear reactions at high energies. First of all, the cross sections and recoil data obtained for 0.6 GeV protons will be analyzed; then the results obtained at 10.5 and 21 GeV will be addressed.

A. 0.6 GeV

1. *Cross sections*

Our cross sections for rubidium and values taken from the literature for the same targets, are given in Table VI. The present results and those of Kruger and Sugarman[44] for ^{86}Rb formed in various targets irradiated at 450 MeV are in satisfactory agreement when the energy difference is taken into account (as well as the minimum error of 30% estimated by Kruger and Sugarman). Comparison of our results for ^{84}Rb and ^{86}Rb in uranium and thorium targets (see Table III) with those of Friedlander *et al.*[2] or Franz and Friedlander[45] (see Table VI) shows that our cross sections are about 20 to 30% higher for energies of the same order. This difference is probably accounted for the different monitoring systems used and by our maximum global error of 30%.

When the cross sections for the three isotopes of Rb are examined as a function of the mass of the target, they are found to diminish exponentially to approximately the region of praseodymium, then to increase from terbium to uranium. The slope of these variations is very marked at 0.6 GeV, but much less so for 10.5 and 21 GeV, as can be seen in Fig. 2. (Only the results for ^{84}Rb are indicated, since they show the average behavior of the three isotopes.)

Also shown in Fig. 2 are the cross sections for ^{84}Rb obtained from the semi-empirical relation of Rudstam[5] for the following targets: ^{89}Y, ^{93}Nb, ^{103}Rh, ^{108}Ag, ^{122}Sb, ^{127}I, ^{141}Pr, and ^{159}Tb. The values thus obtained are shown as crosses for 0.6 GeV and as circles for 10.5 GeV. They have been joined by a continuous line which illustrates the exponential decrease of cross sections with increasing target mass. For 0.6 GeV, good agreement is found between experimental and calculated values, from yttrium to praseodymium, inclusive. With a terbium target, on the contrary, a factor of 30 is found between the experimental cross sections and those calculated by means of the semi-empirical formula.

In the following paragraph, the recoil experi-

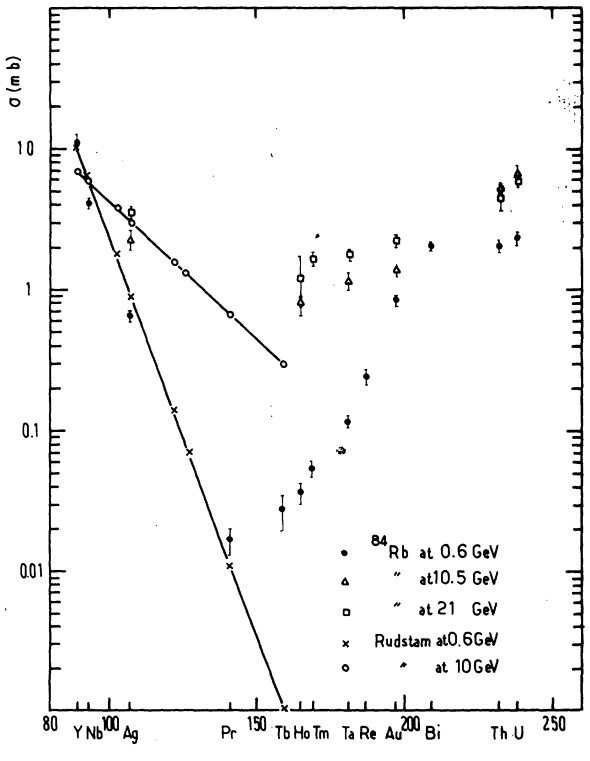

FIG. 2. The dependence of cross sections on target mass for ^{84}Rb at 0.6, 10.5, and 21 GeV.

ments will be examined in an attempt to account for the formation of rubidium in various targets and, particularly, in the rare earths. Unfortunately, it has been impossible to carry out such experiments with praseodymium, where the cross sections obtained at 0.6 GeV suggest a spallation mechanism. Very long irradiation times are required for recoil experiments with praseodymium and the easily oxidized target disaggregates into a fine powder.

2. *Recoil data*

The recoil properties that we observe confirm the presence of at least two processes in the formation of the rubidium isotopes at 0.6 GeV. (See Table VII.) With changes in target they show marked differences in the ranges (i.e., the momenta or the kinetic energies in the recoil system), the excitation energies, and the mean momentum per emitted nucleon. The results for different targets can be classified in three separate groups: Y, Nb, Ag; then Tb, Ho, and finally Ta, Re, Au, Bi, Th, and U.

The spallation mechanism suggested by the exponential decrease of cross sections with increasing ΔA is confirmed by the recoil experiments for the group Y, Nb, Ag. In a study of the velocities of the products of deep spallation, Crespo, Cumming, and Alexander[47] established an empirical relation which can be used, in principle, to distinguish between fission and spallation. They relate the mean squared momentum per evaporated nucleon to the mass of the target, A_t, that of the observed product, A_{obs}, and its mean kinetic energy, $\langle T\rangle$, in the center of mass sytem, by the relation

$$\langle m_i{}^2 v_i{}^2\rangle = \frac{(A_{obs}+A_t)^2\langle T\rangle}{2A_{obs}(A_t - A_{obs})} . \qquad (2)$$

The order of magnitude of the mean squared momentum in spallation can be deduced from the mean kinetic energy per nucleon evaporated. When ΔA varies from 10 to about 30, it may be reasonably estimated[48,49] that the energies of excitation

TABLE VII. Recoil data for various targets and 0.6 GeV protons.

Target (product)	R (mg/cm^2)	N	$\langle T\rangle$ (MeV)	$\langle P\rangle$ [(MeV/u)$^{1/2}$]	E^* (MeV)	$\langle T\rangle/\bar{E}$	$\langle m_i^2 v_i^2\rangle$ (MeV/u)	Mechanism
Y (^{83}Rb)	0.26 ± 0.01	1.97	1.3 ± 0.1 (7%)	14.6 ± 0.3	63 ± 5	1.04 ± 0.05	29	S_I
(^{84}Rb)	0.23 ± 0.01	1.97	1.2 ± 0.1 (8%)	14.3 ± 0.2	56 ± 3	0.96 ± 0.02	35	S_I
Nb (^{83}Rb)	0.45 ± 0.04	1.88	2.5 ± 0.2 (12%)	20.3 ± 0.7	107 ± 14	2.01 ± 0.16	37	S_I
(^{84}Rb)	0.41 ± 0.03	1.88	2.1 ± 0.2 (14%)	18.8 ± 0.8	86 ± 14	1.69 ± 0.16	41	S_I
Ag (^{83}Rb)	0.94 ± 0.03	1.70	4.5 ± 0.2 (27%)	27.3 ± 0.6	182 ± 13	0.35 ± 0.01	35	S_I
(^{84}Rb)	0.84 ± 0.05	1.70	4.0 ± 0.3 (27%)	25.9 ± 0.9	169 ± 21	0.31 ± 0.02	36	S_I
Tb (^{83}Rb)	2.8 ± 0.5	1.40	11.3 ± 1.3 (13%)	43.1 ± 2.5	118 ± 76	0.21 ± 0.02	52	S_{II}
(^{84}Rb)	3.3 ± 1.3	1.34	16 ± 5 (26%)	52.0 ± 8.1	109 ± 76	0.30 ± 0.08	76	S_{II}
Ho (^{83}Rb)	3.6 ± 0.2	1.35	17 ± 1 (13%)	53.1 ± 1.6	151 ± 43	0.28 ± 0.01	76	S_{II}
(^{84}Rb)	4.5 ± 1.6	1.19	25 ± 8 (26%)	64.7 ± 10.4	183 ± 135	0.49 ± 0.12	115	S_{II}
Ta (^{83}Rb)	7.1 ± 0.1	1.07	56 ± 2 (12%)	96.4 ± 1.6	334 ± 23	0.80 ± 0.02	239	F
(^{84}Rb)	8.7 ± 0.2	1.05	77 ± 3 (16%)	113.6 ± 2.1	332 ± 26	1.10 ± 0.04	331	F
Re (^{83}Rb)	7.5 ± 0.9	1.06	57 ± 12 (14%)	97.1 ± 10.0	250 ± 61	0.81 ± 0.17	241	F
(^{84}Rb)	8.5 ± 0.3	1.05	72 ± 5 (16%)	109.8 ± 3.7	374 ± 57	1.03 ± 0.07	306	F
Au (^{83}Rb)	7.9 ± 0.2	1.06	61 ± 3 (12%)	100.6 ± 2.4	306 ± 43	0.76 ± 0.03	252	F
(^{84}Rb)	9.1 ± 0.2	1.04	77 ± 3 (14%)	113.7 ± 2.3	232 ± 29	0.96 ± 0.04	320	F
(^{86}Rb)	10.0 ± 0.4	1.04	82 ± 7 (1%)	118.8 ± 5.0	242 ± 45	1.03 ± 0.09	343	F
Bi (^{83}Rb)	8.4 ± 0.4	1.04	63 ± 5 (11%)	102.3 ± 4.0	282 ± 43	0.79 ± 0.06	256	F
(^{84}Rb)	8.9 ± 0.1	1.04	70 ± 2 (11%)	108.5 ± 1.5	251 ± 20	0.87 ± 0.02	285	F
(^{86}Rb)	10.0 ± 0.3	1.04	78 ± 5 (4%)	115.7 ± 3.7	207 ± 38	0.98 ± 0.06	320	F
Th (^{83}Rb)	10.5 ± 0.5	1.02	87 ± 8 (11%)	120.3 ± 5.3	336 ± 63	0.89 ± 0.08	349	F
(^{84}Rb)	10.3 ± 0.2	1.02	83 ± 4 (10%)	118.2 ± 2.8	242 ± 22	0.85 ± 0.04	333	F
(^{86}Rb)	10.3 ± 0.4	1.02	81 ± 7 (11%)	118.2 ± 5.0	250 ± 48	0.83 ± 0.07	326	F
U (^{83}Rb)	10.8 ± 0.3	1.02	86 ± 5 (12%)	119.4 ± 3.4	270 ± 44	0.86 ± 0.05	344	F
(^{84}Rb)	10.7 ± 0.4	1.02	85 ± 6 (11%)	119.4 ± 4.0	263 ± 43	0.85 ± 0.06	340	F
(^{86}Rb)	10.9 ± 0.6	1.02	89 ± 9 (11%)	123.7 ± 6.0	207 ± 43	0.89 ± 0.09	357	F

necessary for such evaporation chains fall in the interval of 100 to 300 MeV for spallation. With an exit barrier of 10 MeV for the protons and approximately the same number of protons and neutrons evaporated, the mean squared momentum per nucleon evaporated corresponding to such excitation energies falls approximately in the range of 20 to 40 MeV u. These expected values agree with those found here for the targets Y, Nb, and Ag. The foregoing rough estimation obscures the relation independent of E_p, which exists between $\langle P\rangle$ and ΔA. That relation will be discussed later.

When the target is lighter than silver, the ranges are inferior to 1 mg/cm^2 at 0.6 GeV, whereas values of 3 to about 5 mg/cm^2 are observed with the rare earths. With the rare earth targets, the value of N (from Ref. 36) in the range-energy relations is found to lie in the interval 1.20 to 1.40. On passing from tantalum to uranium, R increases from 7 to 11 mg/cm^2. The value of N for this entire group is of the order of 1. Particularly interesting is the variation of the mean squared momentum per nucleon evaporated, $\langle m_i^2 v_i^2\rangle$, with the nature of the target, i.e., ΔA. While it is of the order of 30 to 40 MeV u for the group Y, Nb, Ag (corresponding to "type S_I" spallation with ejection of several nucleons during the cascade), it is found to be about 50 to 120 MeV u for the rare earths and reaches 250 to 350 MeV u from tantalum to uranium. Keeping in mind the approximate nature of the formula, the precise value of $\langle m_i^2 v_i^2\rangle$ obtained is of less interest than its use as a test for spallation. When the nuclear temperatures are calculated as functions of $\langle m_i^2 v_i^2\rangle$, excessive temperatures are obtained for values higher than 50 MeV u. In spite of the various approximations, an additional velocity, other than that of the nucleons evaporated during spallation, must be envisaged, e.g., arising from fission or another mechanism.

A good test for fission F may be made by comparing the experimental kinetic energies, $\langle T\rangle$, with those calculated theoretically, $\overline{E}$, by Nix and Swiatecki[27] according to the liquid drop model. The expected ratio should generally be less than unity, since, in the calculation, the fissioning nucleus is equated with the target nucleus (we neglect the mass difference due to nucleons lost during the prompt cascade and to prefission evaporation). If the results for the light-target group are excluded (Y, Nb, Ag), the ratio $\langle T\rangle/\overline{E}$ is found to lie between 0.76 and 1.10 for the targets U, Th, Bi, Au, Re, and Ta. The fluctuations do not appear to be incompatible with the hypothesis of a fission mechanism. The deduced excitation energy E^* increases from uranium to tantalum and may be expected to be correlated with the fission barriers and saddle-point shapes. If extensive deformations ensue, the observed values of $\langle T\rangle$ may no longer correspond exactly to the approximations of the calculations. However, it seems that, independently of the variations of $\langle T\rangle/\overline{E}$, the main body of results obtained for the formation of ^{83}Rb and ^{84}Rb at 0.6 GeV in Ta, Re, Au, Bi, Th, and U suggests a fission process. The cross sections increase very rapidly with the target mass, indicating, among other things, an increase of the fissionability. The highest excitation energies, E^* (within the uncertainties) are observed for the highest fission barriers. In order that fission become a process competitive with evaporation in the deexcitation of a cascade nucleus formed by a target such as tantalum, there must be an increase in the excitation energy and therefore of the nuclear temperature. The latter influences the fission width, and therefore $\Gamma_f/(\Gamma_n+\Gamma_f)$, by its effect on the barrier, which may be estimated from the lowering of the nuclear surface energy.[50]

With rare-earth targets, values of $\langle T\rangle/\overline{E}$ are found to fall within the range 0.20 to 0.50. Even assuming that the fission model used is not quite correct in this case, due to the various approximations, it should nevertheless be noted that the apparent excitation energies here are lower by a factor of 2 or 3 compared with those obtained with tantalum targets. This result is in disagreement with the preceding conclusions concerning the influence of E^* on the fissionability. In addition, if the rubidium from the terbium and holmium targets is assumed to be produced by spallation, a disagreement is found between the nuclear temperatures deduced from the values of $\langle m_i^2 v_i^2\rangle$ (greater than 50 MeV u) and those one might obtain using the excitation energies determined by Eq. (1). It would thus appear that the results for the rare earths are inconsistent when analyzed from the point of view of either pure fission F or pure spallation S_I.

The present results for rubidium production in various targets at 0.6 GeV may be compared with those of Kaufman, Steinberg, and Weisfield[1] for the production of several isotopes in gold at 1 GeV. Figure 3 shows the values of $\langle P\rangle = A\langle V\rangle$ for common values of ΔA. The theoretical curves correspond to fission and spallation in gold targets. The present results are shown as squares and triangles, those of Kaufman, Steinberg, and Weisfield as circles.

The mean momenta observed with Y, Nb, and Ag targets (Fig. 3) are slightly higher than those observed with Au for the same ΔA. Several factors may intervene to account for this difference: first, the difference between target and product mass, multiple scattering corrections, and approximations in the mathematical treatment of the

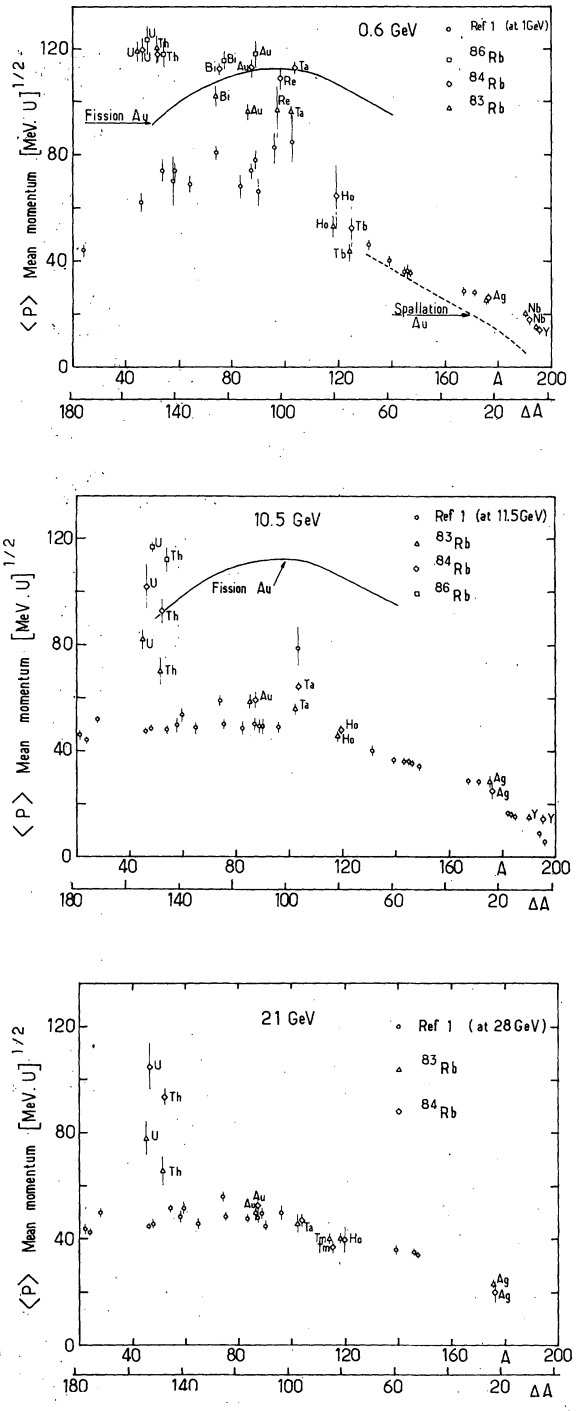

FIG. 3. Mean momenta $\langle P \rangle$ as a function of mass difference from the target ΔA: ○ Kaufman *et al.*, Ref. 1; △ present data for ^{83}Rb; ◇ present data for ^{84}Rb; □ present data for ^{86}Rb. The solid curve shows the momenta for binary fission of Au and the dashed curve the calculated momenta for spallation (see text). (a) Ref. 1 at 1 GeV, our results at 0.6 GeV. (b) Ref. 1 at 11.5 GeV, our results at 10.5 GeV. (c) Ref. 1 at 28 GeV, our results at 21 GeV.

recoil data.

The experimental mean momenta obtained with Ho and Tb targets are of the same order of magnitude as those observed[1] for ^{139}Ce and ^{131}Ba in Au at 1 GeV and, like the latter, are much higher than the theoretical values.

Good agreement is observed between the present values and the theoretical mean momenta for gold target when rubidium is formed in Au, Bi, Re, and Ta, particularly in the case of ^{84,86}Rb, which is produced by pure binary fission. The experimental mean momenta for ^{83}Rb are slightly smaller than the theoretical values, indicating a small contribution from deep spallation. However, the principal mechanism of formation of this isotope must be binary fission. As expected, the experimental mean momenta for the three rubidium isotopes in uranium and thorium targets lie well above the theoretical curve for fission products of the same ΔA produced in gold.

B. 10.5 and 21 GeV

As in the case of the 0.6 GeV results, those obtained at 10.5 and 21 GeV are to be interpreted by comparison with those expected for the mechanisms of spallation and fission. To this end, the experimental results will be compared with calculations based on the two-step model: a cascade with ejection of free nucleons, followed by the deexcitation by fission or evaporation once thermodynamic equilibrium of the excitation energy is reached. In particular, the correlations between the range, R, the fissioning nucleus, and the excitation energy, E^* will be examined.

1. Cross sections

When the cross sections obtained for ^{83}Rb(C) and ^{84}Rb(I) at 10.5 GeV in gold are compared with those obtained by Kaufman *et al.*[8] at 11.5 GeV, the agreement is satisfactory. For the two isotopes, these authors found 6.85 ± 0.49 and 1.75 ± 0.35 mb, respectively, whereas the values obtained here are 6.65 ± 0.12 and 1.41 ± 0.05 mb.

By forming the ratio, $\sigma_{10.5\,\mathrm{GeV}}/\sigma_{0.6\,\mathrm{GeV}}$, of the cross sections at 10.5 and 0.6 GeV, it may be noted that the influence of the incident energy on the isotopic distribution depends on the mass of the target (Fig. 4). Three large zones may be distinguished, between yttrium and uranium:

(a) The targets close to rubidium, such as Y and Ag, give rise to reactions where the incident energy has little influence on the isotopic distribution. The latter is approximately Gaussian and centered in the neighborhood of stability[9,51]; it is neither broadened nor displaced when E_p reaches multi-GeV energies. The excitation functions are prac-

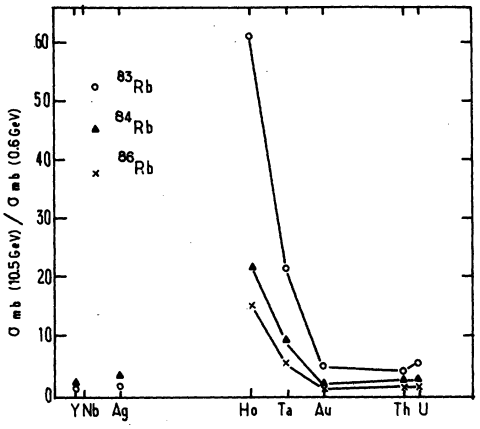

FIG. 4. Cross section ratios (10.5 GeV/0.6 GeV) for product formation in various targets.

tically constant in the interval 0.6 to 10.5 GeV, once the plateau is reached, whether the isotopes are neutron-excessive or deficient. From the comparison of the experimental and calculated cross sections for an energy of several GeV (see Fig. 2), it is not possible to establish with precision the targets beyond which spallation may or may not be proposed (except for Y, Nb, and Ag).

(b) From the rare earths to tantalum, the influence of the incident energy on the cross section ratio is greater, the more the isotope is deficient in neutrons. In Ho targets, the ratio of the cross section at 10.5 to that at 0.6 GeV is 63 for ^{83}Rb, 22 for ^{84}Rb, and 15 for ^{86}Rb (Fig. 4). This gives rise to a noticeable widening of the isotopic distribution towards more neutron deficiency, accompanied by a displacement of the maximum in the same direction. For the case of tantalum, Trabitzsch and Bächmann[25] observed, for the isobar $A=86$, a charge dispersion which was practically Gaussian, with a maximum which shifted from $N/Z=1.263$ to 1.216 and a width from 1.85 units of Z to 1.93, when the incident energy was changed from 580 MeV to 19 GeV. The excitation functions for ^{83}Rb and ^{86}Rb increase with E_p between 0.6 and 21 GeV.

(c) From gold to uranium, the relative rate of production of an isotope is very sensitive to its position with respect to the stability line. From gold to uranium, the ratio of the cross sections at 10.5 and 0.6 GeV shifts from 4.7 to 5.9 for ^{83}Rb, from 1.6 to 2.8 for ^{84}Rb and remains in the neighborhood of unity for ^{86}Rb. This variation with E_p corresponds, in the isotopic distribution, to the formation of a second maximum associated with the neutron-deficient isotopes,[7] whereas the absolute values and even the width of the distribution remain practically unchanged on the neutron-excess side of the stability line. In the interval considered, the excitation functions are increasing for the deficient isotopes and constant or decreasing for the neutron-excess ones. For the isotopes close to stability, the excitation functions are intermediate in form, with a maximum at about 1 GeV.[2]

2. *Recoil results*

Tables VIII and IX show the values of R, N, $\langle T\rangle$, $\langle P\rangle$, E^*, $\langle T\rangle/\bar{E}$, and $\langle m_i^2 v_i^2\rangle$ obtained at 10.5 and

TABLE VIII. Recoil data for various targets and 10.5 GeV protons.

Target (product)	R (mg/cm^2)	N	$\langle T\rangle$ (MeV)	$\langle P\rangle$ [(MeV/u)$^{1/2}$]	E^* (MeV)	$\langle T\rangle/\bar{E}$	$\langle m_i^2 v_i^2\rangle$ (MeV/u)	Mechanism
Y (^{83}Rb)	0.28 ± 0.02	1.97	1.5 ± 0.1 (6%)	15.8 ± 0.5	52 ± 6	1.20 ± 0.08	29	S_I
(^{84}Rb)	0.25 ± 0.01	1.97	1.3 ± 0.1 (8%)	14.8 ± 0.6	42 ± 5	1.04 ± 0.07	35	S_I
Ag (^{83}Rb)	1.03 ± 0.14	1.66	5.2 ± 0.8 (13%)	29.3 ± 2.1	127 ± 28	0.41 ± 0.06	43	S_I
(^{84}Rb)	0.80 ± 0.11	1.75	3.8 ± 0.6 (24%)	25.2 ± 2.0	111 ± 23	0.30 ± 0.05	27	S_I
Ho (^{83}Rb)	3.1 ± 0.2	1.34	13 ± 1 (28%)	46.5 ± 1.7	201 ± 33	0.22 ± 0.02	58	S_{II}
(^{84}Rb)	3.2 ± 0.1	1.34	14 ± 1 (28%)	48.5 ± 1.0	179 ± 22	0.23 ± 0.01	63	S_{II}
Ta (^{83}Rb)	3.9 ± 0.1	1.31	19 ± 1 (1%)	56.1 ± 1.2	163 ± 23	0.27 ± 0.01	81	S_{II}
(^{84}Rb)	4.6 ± 0.1	1.23	25 ± 1 (8%)	64.8 ± 0.7	187 ± 8	0.35 ± 0.01	107	S_{II}
Au (^{83}Rb)	4.2 ± 0.1	1.28	20 ± 1 (5%)	57.6 ± 1.4	152 ± 17	0.25 ± 0.01	82	S_{II}
(^{84}Rb)	4.6 ± 0.3	1.26	21 ± 2 (5%)	59.4 ± 2.8	158 ± 22	0.26 ± 0.02	87	S_{II}
Th (^{83}Rb)	5.9 ± 0.5	1.18	30 ± 4 (1%)	70.5 ± 4.6	132 ± 26	0.30 ± 0.04	120	S_{II}
(^{84}Rb)	7.5 ± 0.4	1.05	52 ± 5 (9%)	93.5 ± 4.2	139 ± 26	0.53 ± 0.05	208	$S_{II}+F$
(^{86}Rb)	9.5 ± 0.4	1.02	74 ± 7 (11%)	112.7 ± 5.9	184 ± 36	0.79 ± 0.07	299	F
U (^{83}Rb)	7.3 ± 0.3	1.10	41 ± 3 (2%)	82.5 ± 3.0	143 ± 33	0.41 ± 0.03	164	$S_{II}+F$
(^{84}Rb)	8.7 ± 0.7	1.03	63 ± 10 (9%)	102.7 ± 8.0	145 ± 43	0.63 ± 0.10	252	$S_{II}+F$
(^{86}Rb)	10.8 ± 0.1	1.02	81 ± 2 (10%)	117.9 ± 1.5	150 ± 11	0.80 ± 0.02	326	F

TABLE IX. Recoil data for various targets and 21 GeV protons.

Target (product)	R (mg/cm^2)	N	$\langle T\rangle$ (MeV)	$\langle P\rangle$ [(MeV/u)$^{1/2}$]	E^* (MeV)	$\langle T\rangle/\bar{E}$	$\langle m_i^2 v_i^2\rangle$ (MeV/u)	Mechanism
Ag (^{83}Rb)	0.70 ± 0.05	1.78	3.4 ± 0.3 (18%)	23.7 ± 1.0	102 ± 17	0.26 ± 0.02	26	S_I
(^{84}Rb)	0.74 ± 0.17	1.78	3.6 ± 0.9 (25%)	24.6 ± 3.0	102 ± 41	0.28 ± 0.07	27	S_I
Ho (^{83}Rb)	2.3 ± 0.1	1.50	10 ± 1 (20%)	40.7 ± 1.4	179 ± 18	0.17 ± 0.01	45	S_{II}
(^{84}Rb)	2.4 ± 0.4	1.50	10 ± 2 (20%)	41.0 ± 4.0	189 ± 25	0.17 ± 0.03	45	S_{II}
Tm (^{83}Rb)	2.3 ± 0.1	1.50	10 ± 1 (10%)	40.7 ± 1.8	195 ± 48	0.16 ± 0.01	44	S_{II}
(^{84}Rb)	2.0 ± 0.2	1.59	8.4 ± 0.9 (7%)	37.5 ± 1.9	198 ± 34	0.13 ± 0.01	35	S_{II}
Ta (^{83}Rb)	3.1 ± 0.3	1.42	13 ± 2 (15%)	46.4 ± 3.5	205 ± 54	0.18 ± 0.03	55	S_{II}
(^{84}Rb)	3.1 ± 0.1	1.42	13 ± 1 (15%)	47.0 ± 1.6	189 ± 23	0.18 ± 0.01	56	S_{II}
Au (^{83}Rb)	3.6 ± 0.3	1.40	16 ± 2 (12%)	51.5 ± 3.1	159 ± 69	0.20 ± 0.03	66	S_{II}
(^{84}Rb)	4.1 ± 0.4	1.32	18 ± 2 (6%)	55.0 ± 3.0	206 ± 63	0.22 ± 0.02	74	S_{II}
Th (^{83}Rb)	5.4 ± 0.5	1.20	26 ± 4 (11%)	65.7 ± 5.0	96 ± 37	0.26 ± 0.04	104	S_{II}
(^{84}Rb)	7.6 ± 0.2	1.02	53 ± 3 (9%)	94.2 ± 2.6	96 ± 9	0.54 ± 0.03	212	$S_{II} + F$
U (^{83}Rb)	6.9 ± 0.7	1.12	37 ± 7 (8%)	78.3 ± 7.3	90 ± 23	0.37 ± 0.07	148	$S_{II} + F$
(^{84}Rb)	9.4 ± 0.7	1.03	66 ± 9 (9%)	105.2 ± 7.6	80 ± 20	0.66 ± 0.09	264	$S_{II} + F$

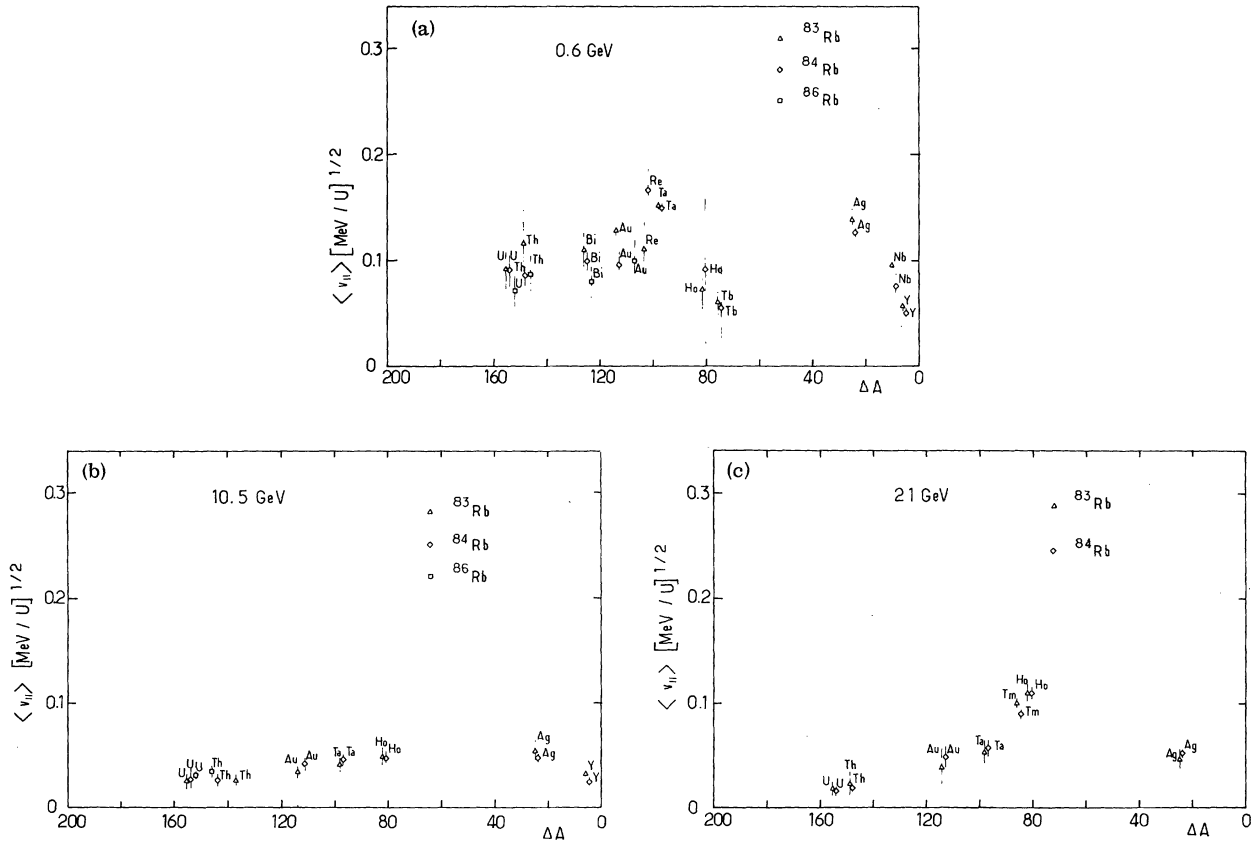

FIG. 5. Mean cascade velocity $\langle v_{II}\rangle$ as a function of product-target mass difference, ΔA. (a) 0.6 GeV, (b) 10.5 GeV, (c) 21 GeV.

21 GeV. Characteristic changes with respect to 0.6 GeV concern essentially the decrease of the range and of the apparent excitation energy of the neutron-deficient isotopes in certain targets. For targets from tantalum to uranium, the range of ^{83}Rb falls by about a factor of 2 when the incident energy is increased from 0.6 to 10.5 GeV. The range of the isotope 84 changes in the same way with energy, except for the targets thorium and uranium, where the diminution is only by a factor of about 1.3. The range of ^{86}Rb, on the contrary, remained unchanged in those targets where the experimental conditions allowed it to be detected (thorium and uranium). Also unchanged were the ranges of ^{83}Rb and ^{84}Rb produced in the rare earths. At 21 GeV, the ranges are noticeably shorter than those observed at 10.5 GeV. Similar results for R and E^* have been observed at 11.5 GeV[10] with uranium targets and at 18 GeV[26] with tantalum targets for the isotopes ^{131}Ba, ^{83}Sr, and ^{83}Rb.

Mean momenta $\langle P \rangle$. At 10.5 and 21 GeV the momenta are smaller than at 0.6 GeV (see Fig. 3) for neutron-deficient isotopes, in targets heavier than rare earths, indicating a smaller fission contribution at the higher energy. This high energy mechanism is generally termed deep spallation and probably involves emission of light fragments. In the case of rubidium formed in Y, Nb, Ag, and Ho, on the other hand, there is no evident energy dependence, implying no change in mechanism between 0.6 and 21 GeV.

Cascade velocities and excitation energy. Figures 5(a), 5(b), 5(c) show $\langle v_{\parallel} \rangle$, the mean cascade velocity in the beam direction, obtained from the recoil data, as a function of ΔA for each incident energy.

The variation of $\langle v_{\parallel} \rangle$ with ΔA is similar to that observed by Kaufman, Steinberg, and Weisfield.[1] The calculation of $\langle v_{\parallel} \rangle$ for spallation, using the Vegas and ORNL model[52,53] considerably overestimates $\langle v_{\parallel} \rangle$ for $\Delta A > 60$ in the case of gold targets. A fission mechanism must be excluded, however, given the momenta values. Our results for $\langle v_{\parallel} \rangle$ and $\langle P \rangle$ in the case of rubidium formed in Ho at the three incident energies lead to the same conclusion.

In Fig. 6 we see no dependence on bombarding energy for the formation of near spallation products. Also, we see a decrease in the apparent values of E^* (from relation 1) with increasing incident energy.

Next, we shall try to interpret the foregoing behavior by examining the factors which have a bearing on the mechanisms of fission or spallation. First, we eliminate ^{86}Rb from the discussion, since its production in thorium and uranium seems

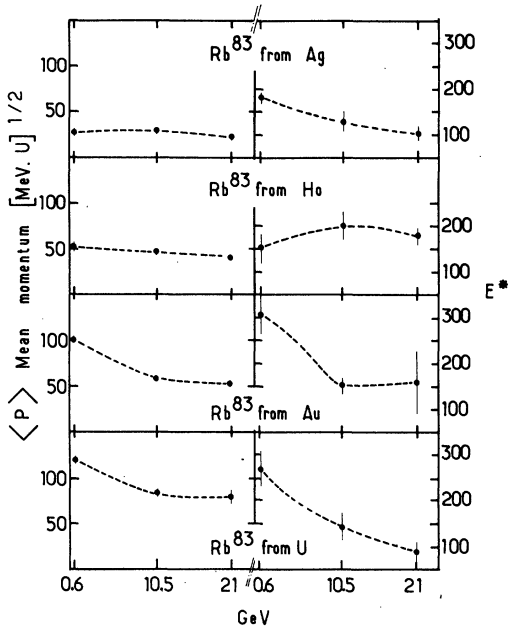

FIG. 6. Variation of the mean momenta $\langle P \rangle$ and excitation energy E^* for the deficient neutron isotope ^{83}Rb with incident proton energy in four targets: Ag, Ho, Au, and U.

to be in good agreement with a binary fission mechanism at medium energy. The excitation energy, E^*, of the residual cascade nuclei leading to ^{86}Rb is only slightly smaller for 10.5 than it is for 0.6 GeV. The $\langle v_{\parallel} \rangle$-$E^*$ relations established by the calculations of Metropolis *et al.*[48] up to an energy of 1.8 GeV can be reasonably extrapolated to 10.5 GeV for this neutron-excess isotope.

3. *Range and mass of the fissioning nucleus*

According to a fission hypothesis, ranges of the order of 6 to 7 mg/cm^2 for ^{83}Rb in uranium at energies of 10.5 and 21 GeV [or $\langle P \rangle$ about 80 (MeV u)$^{1/2}$] would correspond to a fissioning nucleus of mass of about 150. It would seem worth examining the effect of cascade and prefission evaporation with about 90 nucleons, especially since it would correspond to a high probability, at high energy, in the distribution of fissioning nuclei in heavy targets. For this reason, an attempt has been made to characterize the average fissioning nucleus as a function of the energy of excitation, using available calculations.[48,49] The results obtained for a cascade nucleus of ^{229}Th are to be found in Table X. For an excitation energy of 600 MeV associated with about 12 cascade nucleons, one finds, on the average, 34 nucleons evaporated before fission. In the case of a fissioning nucleus of mass of about 150, it would thus require excita-

TABLE X. Total evaporated nucleons i and ratio of neutrons to protons evaporated before fission for the cascade nucleus ^{229}Th as a function of the excitation energy E^*.

E^* (MeV)	100	200	300	400	600
i before fission	7	12	16	20	34
n/p	16.0	8.6	6.4	5.4	3.5

tion energies, after the cascade, of 1000 to 1200 MeV. Such values do not appear compatible with statistical equilibrium and are far from agreement with the experimental values obtained, so that the hypothesis of a fissioning nucleus of mass of about 150 may be excluded.

4. Kinetic energy of a fission fragment and excitation energy of the cascade nucleus

The increasing probability of asymmetric fission with increasing incident energy has been demonstrated by the widening of the distribution of track lengths of the fragments.[54] Let us examine the influence of the excitation energy and of the fractional division of mass on the velocity of the fission fragments. The nuclear reaction leading from the target nucleus, A_t, to the observed product, A_{obs}, may be broken down as follows. First of all, a nucleus A_{casc} is formed after the prompt cascade, then, after emission of i particles, the fissioning nucleus, A_f. The latter gives the primary fragment, A_1, and finally the observed product, after post-fission evaporation of j particles. The resulting velocity, V, corresponding to the second step in the model of Serber, can be written as a function of the velocity due to fission, V_f, and the recoil velocities V_i and V_j due to prefission and postfission evaporation. V can be readily evaluated for the cases of isotropic or symmetrical distributions of the three vectors.

The velocities V_i and V_j are related to $\langle m_{ij}{}^2 v_{ij}{}^2 \rangle$ by the intermediate equation (2). Judging by the experimental results, 25 MeV u appears to be an acceptable approximation for the mean square momentum per evaporated nucleon.

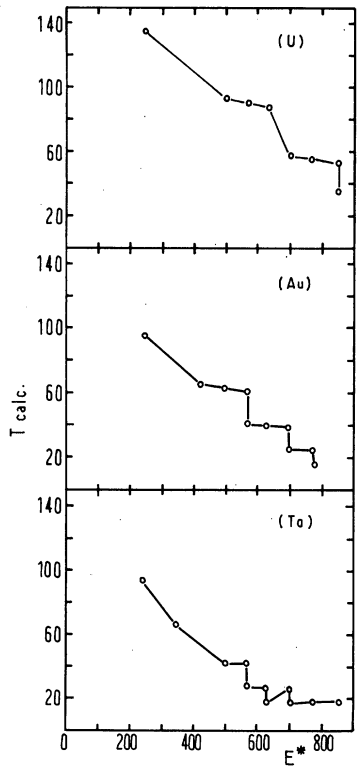

FIG. 7. Calculated kinetic energy T_{calc} [MeV] for ^{83}Rb as a function of the excitation energy of the cascade nucleus E^* in U, Au, and Ta targets.

The fission-fragment velocity, V_f, is a function of the charge Z_f, the mass, A_f, and the mass division $U = A_1/A_f$. Now the charge, Z_f, may be expressed as a function of the mass A_f, beginning with the data of Table X. The latter has been compiled from the results of an earlier calculation[49] concerning the cascade nucleus of ^{229}Th and gives the number of nucleons evaporated before fission, as well as the ratio of neutrons to protons, for a range of excitation energies from 100 to 600 MeV. Under these conditions, the observed fission-fragment velocity, V_f, may be approximated by the following equation:

$$\langle V^2 \rangle = \frac{100(A_t - A_f)}{(A_t + A_f)^2} + 100\,\frac{UA_f - A_{obs}}{(UA_f - A_{obs})^2} + \left(\frac{2e^2}{r_0}\right)\frac{(1-U)^2}{A_f{}^{4/3}U^{1/3}(1-U)^{1/3}}\left[Zt + 1 - \frac{A_t - A_f}{27\exp[-0.077(A_t - A_f) + 2]}\right]^2 \quad (3)$$

A computer program has been employed with the above equation to give values of $\langle V^2 \rangle$ and therefore the kinetic energy, T_{calc}, for ^{83}Rb supposedly formed by fission in targets ranging from the rare earths to uranium. The results of the calculation are to be found in Fig. 7, which shows the variation of T with the excitation energy, E^*, for the cases of uranium, gold, and tantalum. The only explana-

tion for a diminution of R in the hypothesis of fission preceded by a cascade of nonbound nucleons requires an increase of several hundred MeV of the excitation energy, E^*. Regardless of the various approximations employed in the expression for $\langle V^2 \rangle$, it has not been possible to associated a diminishing or even a constant E^* with a diminution of the kinetic energy $\langle T \rangle$.

V. INTERPRETATION

The preceding analysis shows that a contradiction appears when the production of neutron-deficient isotopes is attributed to a model consisting of a cascade, ejecting only nucleons, and a statistical evaporation, pre- or post-fission. However, the apparent contradiction may result from the $\langle v_{\parallel} \rangle$-$E^*$ relations. Their overall validity at incident energies up to several GeV cannot be trusted. Firstly, we have clearly identified the production of ^{83}Rb and ^{84}Rb in Y, Nb, and Ag as resulting from simple spallation, S_I. The excitation energies determined at 10.5 GeV for these targets, although slightly inferior to those at 0.6 GeV, are compatible with the proposed mechanism. Secondly, the result obtained for the E^* values of the cascade nuclei giving ^{86}Rb from thorium and uranium show that the $\langle v_{\parallel} \rangle$-$E^*$ relations cannot be precisely extrapolated to 10.5 GeV, but they do lead to consistent results suggesting a process of binary fission F at medium energies. The cascades leading to the formation of neutron-deficient and neutron-excess isotopes

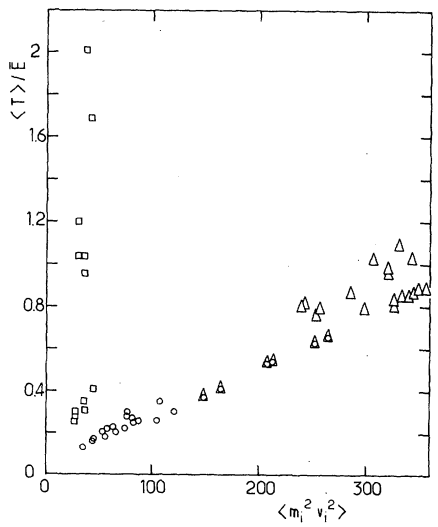

FIG. 8. Ratio of experimental mean kinetic energy, $\langle T \rangle$, to the calculated kinetic energy, $\bar{E}$ (Nix *et al.*, Ref. 27, liquid drop model) versus the mean squared momentum per emitted nucleon, $\langle m_i^2 v_i^2 \rangle$: □ spallation (S_I); ○ deep spallation (S_{II}); △ fission (F); ▲ mixed ($S_{II} + F$).

are not the same with heavy targets. Consequently, the $\langle v_{\parallel} \rangle$-$E^*$ relations can lead to erroneous values of E^*, regardless of the incident energy, for products resulting from particular cascades, not taken into account in the calculation of E^* (such as those corresponding to the ejection of clusters). Moreover, the low values of E^* obtained with rare earth targets give evidence of the above effect for incident energies as low as 0.6 GeV. In our treatment of the recoil data, v was taken to be $v_{\parallel}$. It may be supposed that $v_{\perp}$ has been underestimated. In any case, taking $v_{\perp}$ into account would constitute only a minor correction.

With the above conclusions in mind, we propose an interpretation of our results involving three mechanisms, suggested by the variations of R, $\langle P \rangle$, $\langle v_{\parallel} \rangle$, and E^* with E_p and by the plot of $\langle T \rangle / \bar{E}$ versus $\langle m_i^2 v_i^2 \rangle$ (experimental kinetic energy $\langle T \rangle$ deduced from recoil experiments divided by $\bar{E}$, the calculated energy from the liquid drop model, versus the mean square momentum $\langle m_i^2 v_i^2 \rangle$ corresponding to the same rubidium isotope; see Fig. 8).

1. Spallation, S_I

This process corresponds to the classical model of spallation with a cascade ejecting several nucleons, followed by a statistical evaporation of nucleons and clusters up to α particles. The range R is only slightly influenced by the incident energy. The mean square momentum per nucleon evaporated, $\langle m_i^2 v_i^2 \rangle$, is of the order of 25 to 40 MeV u. The excitation energy, E^*, increases with ΔA for a given target and product, but is not very sensitive to the incident energy. On the diagram of $\langle T \rangle / \bar{E}$ versus $\langle m_i^2 v_i^2 \rangle$, the points associated with such nuclear reactions correspond to the production of ^{83}Rb and ^{84}Rb in yttrium, niobium, and silver targets at incident energies of 0.6, 10.5, and 21 GeV. The points are indicated by squares and fall on a straight line on Fig. 8.

2. Medium energy fission, F

This process denotes a binary fission occurring during the deexcitation of a cascade nucleus from a heavy target (beyond the rare earths), disposing of an excitation energy of several tens of MeV up to about 300 MeV, after ejection of the cascade nucleons. The mass distribution of the fragments of such fission is symmetrical and centered on a mass of about one-half that of the target. This process is presumably responsible for the formation of the isotopes 83 and 84 of rubidium at 0.6 GeV in targets of tantalum, rhenium, gold, bismuth, thorium, and uranium.

The ratio F/B increases from 1.3 to 1.7 for targets from uranium to tantalum. In parallel with

this increase of F/B, an increase in E^* is noted, showing the incidence of higher and higher fission barriers. The fission process, F, is not very different for incident energies of several GeV than for 0.6 GeV. The range of a fission product such as ^{86}Rb in uranium and thorium is about 3 to 5% shorter at 10.5 GeV than at 0.6 GeV. The ratio between the experimental and calculated kinetic energies is also close to 1. As expected, $\langle m_i^2 v_i^2 \rangle$ reaches exceptionally high values, lying between 250 and 350 MeV u. The corresponding points on the $\langle T \rangle / \overline{E}$ versus $\langle m_i^2 v_i^2 \rangle$ diagram are represented by triangles and lie on the right-hand side of Fig. 8.

3. *Deep spallation, S_{II}*

This process is proposed to account for the formation of ^{83}Rb and ^{84}Rb in holmium and terbium targets at incident energies from 0.6 GeV upwards, since all of the experimental results cannot be reconciled with the mechanism S_I. As for the process S_I, the range and the excitation energies in these cases are similar for the three incident energies. The values of $\langle m_i^2 v_i^2 \rangle$, however, lie between 50 and 120 MeV u. They increase more rapidly than predicted by the relation which gives the variation of the mean square momenta with ΔA,[47] established for spallation reactions where ΔA lies between 25 and 65 u. But, above all, the values of E^* obtained from the $\langle v_\parallel \rangle$-$E^*$ relations lead to energies per evaporated nucleon of the order of 2 to 4 MeV/nucl. These observations give rise to the hypothesis of a "deep" spallation, S_{II}, which differs from S_I by the cascade process, which involves the ejection of nuclear clusters emitted preferentially in the forward direction. The above mechanism might also account for the formation of the isotopes ^{83}Rb and ^{84}Rb at 10.5 and 21 GeV from Ho, Tm, Ta, Re, Au, and for ^{83}Rb in thorium at these energies. The values of R are different from those obtained at 0.6 GeV for the Ta, Re, Au, and Th targets, since the mechanism of production at the latter energy was fission.[1] Thus, between 0.6 GeV and 10.5 GeV, the range falls, on the average, by a factor of 2, accompanied by an apparent diminution of E^* and of F/B (these last two effects reinforce the hypothesis of forward-peaked fragment emission). The values of $\langle T \rangle / \overline{E}$ lie between 0.13 and 0.35. On the other hand, R and E^* appear to be insensitive to the incident energy for rare earth targets when the S_{II} process was observed at energies as low as 0.6 GeV.

4. *Mixed S_{II} and F*

The results in Fig. 8 show that the passage from S_{II} process (lower left) to fission (upper right) is approximately linear as a function of $\langle m_i^2 v_i^2 \rangle$. The nuclear reactions in the intermediate region correspond to the formation of ^{84}Rb in thorium and ^{83,84}Rb in uranium, at 10.5 and 21 GeV, and the ranges are lower only by about 20 to 30%, compared to those observed at 0.6 GeV. The values of $\langle m_i^2 v_i^2 \rangle$ (about 150 to 265) are much higher than those observed for S_{II} spallation and are associated with long ranges, suggesting that an additional velocity has been acquired in a fission-type process during deexcitation. The points in the intermediate region may thus represent a mixture of S_{II} and F processes, the proportions varying with the nature of the target and the isotope.

V. CONCLUSION

The thick-target, thick-catcher recoil technique, radio-chemical methods, and a mathematical analysis have been used to determine certain important characteristics of nuclear reactions. Determinations have been made of the range R, the associated kinetic energy T, the mean momentum $\langle P \rangle$ of the isotopes ^{83}Rb, ^{84}Rb, and ^{86}Rb produced in medium and heavy targets, and the excitation energy E^* of the residual cascade nucleus.

The mean square momentum per evaporated nucleon is used as a test for spallation. In conjunction with the excitation energy, E^*, it permits two types of spallation to be distinguished: (i) spallation, S_I, such that only nucleons, and several deuterons, tritons, and alphas are ejected during the cascade. (ii) deep spallation, S_{II}, where the cascase involves particularly the ejection of fragments, preferentially in the forward direction.

In addition to these spallation processes, there is substantial evidence for binary fission. The ratio of experimental to calculated kinetic energies (as reflected by measured ranges) and the apparent excitation energies suggest a fission mechanism.

Depending on the nature of the target some rubidium formed by fission at 0.6 GeV may be formed by an S_{II} process or a mixture of S_{II} and fission at 10.5 and 21 GeV.

Comparison of the results obtained with protons and with relativistic heavy ions[46,55] may lead to a better understanding of deep spallation and its possible relation to the fireball model.[56,57]

ACKNOWLEDGMENTS

The authors express their gratitude to the coordination teams of the S. C. and of the P. S. of CERN. They would also like to express their appreciation to Dr. S. Regnier for writing the programs, to Dr. A. MacKenzie Peers for help with the manuscript, and to Mr. Brout for his technical collaboration.

APPENDIX

The thick-target, thick-catcher technique (both target and catchers are thick compared to the range of the products of interest) has been used extensively. The analysis of the data is done using the two step vector model[58] in a way first developed by Sugarman and co-workers.[59-61]

The range, R, has been determined from a vector addition scheme. In this model, the mean velocity $\vec{V}_L$ of a product formed in a nuclear reaction may be considered to be the resultant of two independent vectors, $\vec{v}$ and $\vec{V}$. The vector v is the velocity in the laboratory system, resulting from the prompt cascade; $\vec{V}$, in the recoiling center of mass system, corresponds to evaporation or fission (leading to the observed product) during the deexcitation step. In our development, the component of v perpendicular to the beam ($v_\perp$) is neglected and v is taken to be only the component ($v_\parallel$) parallel to the beam. The distribution of $\vec{V}$ is taken to be symmetrical in the recoil system. The relation between the range and the recoil velocity in the two systems can be expressed as follows:

$$R_L = K|\vec{v}+\vec{V}|^N \quad \text{and} \quad R = K'|\vec{V}|^{N'}.$$

K and N depend on the nature of the recoil ion, on its velocity, and on the stopping medium. Empirical values of K and N do not vary much over a restricted velocity interval. In the case of fission, $\vec{v}$ is negligible compared with $\vec{V}$, so that $K' \approx K$ and $N' \approx N$. It has been shown elsewhere[62] that the same approximations can be made in the case of spallation of a target of about mass 50. Considering the expected values of v and V in the spallation of targets of mass 100 to 150, it would seem that the approximations are still reasonable in such cases. Under these conditions, the mathematical treatment of the recoil data for thick target and thick collector enables F and B to be expressed[63] as functions of R, $\eta = v/V$, N, and b/a, the anisotropy parameter:

$$F = \frac{R}{16\eta^4 W(1+b/3a)}\left\{(1+\eta)^{N+1}\left[\frac{4\eta^2}{N+3}(1+\eta)^2 + \frac{4\eta^2}{N+1}(\eta^2-1) + \frac{b}{a}\left(\frac{1}{N+7}(1+\eta)^6 - \frac{\eta^2+3}{N+5}(1+\eta) - \frac{\eta^4-2\eta^2-3}{N+3}(1+\eta)^2 + \frac{(1+\eta^2)^2(\eta^2-1)}{N+1}\right)\right] - (1-\eta^2)^{(N+1)/2}\left[\frac{4\eta^2}{N+3}(1-\eta^2) + \frac{4\eta^2}{N+1}(\eta^2-1) + \frac{b}{a}\left(\frac{1}{N+7}(1-\eta^2)^3 - \frac{(\eta^2+3)(1-\eta^2)^2}{N+5} - \frac{\eta^4-2\eta^2-3}{N+3}(1-\eta^2) + \frac{(1+\eta^2)^2(\eta^2-1)}{N+1}\right)\right]\right\};$$

B is obtained by changing η to $-\eta$.

The range, R, and the associated value of η are determined by means of a program which compares the experimental and calculated values of f (ratio of the sum to the difference of F and B) differing by less than 1%. This is done, in the isotropic case, by allowing η to vary step by step from 0 to 1 and N from 1 to 2. A first set of values of η and N satisfying the conditions gives a first approach to the value of R (the various values of R thus obtained differ by about 5%). However, R and N are not independent, but are subject to range-energy relations. The tables of Northcliffe-Schilling[36] are used, with the values of R as a function of η and N, to obtain the range, R, coupled with the only acceptable value of N and, consequently, of η. The influence of anisotropy has been examined by giving different values b/a. The effect is not very significant compared with the experimental fluctuations.

[1]S. B. Kaufman, E. P. Steinberg, and M. W. Weisfield, Phys. Rev. C 18, 1349 (1978).
[2]G. Friedlander, L. Friedman, B. Gordon, and L. Yaffe, Phys. Rev. 129, 1809 (1963).
[3]J. M. Alexander, C. Baltzinger, and M. F. Gazdik, Phys. Rev. 129, 1826 (1963).
[4]G. Friedlander, in *Proceedings of the Symposium on the Physics and Chemistry of Fission, Salzburg, 1965* (International Atomic Energy Agency, Vienna, Austria, 1965), Vol. II, p. 265.
[5]G. Rudstam and G. Sørensen, J. Inorg. Nucl. Chem. 28, 771 (1966).

[6]E. Hagebø, J. Inorg. Nucl. Chem. 29, 2515 (1967).
[7]R. Klapisch, J. Chaumont, J. Jastrzebski, R. Bernas, G. N. Simonoff, and M. Lagarde, Phys. Rev. Lett. 20, 743 (1968).
[8]S. B. Kaufman, M. W. Weisfield, E. P. Steinberg, B. D. Wilkins, and D. Henderson, Phys. Rev. C 14, 1121 (1976).
[9]J. Hudis, T. Kirsten, R. W. Stoenner, and O. A. Schaeffer, Phys. Rev. C 1, 2019 (1970).
[10]K. Beg and N. T. Porile, Phys. Rev. C 3, 1631 (1971).
[11]Y. Y. Chu, E. M. Franz, G. Friedlander, and P. J. Karol, Phys. Rev. C 4, 2202 (1971).
[12]Y. W. Yu and N. T. Porile, Phys. Rev. C 7, 1597 (1973).
[13]Y. W. Yu, N. T. Porile, R. Warasila, and O. A. Schaeffer, Phys. Rev. C 8, 1091 (1973).
[14]R. Brandt, *Physics and Chemistry of Fission* (International Atomic Energy Agency, Vienna, 1965), Vol. II, p. 329.
[15]J. A. Panontin and N. T. Porile, J. Inorg. Nucl. Chem. 32, 1775 (1970).
[16]J. B. Cumming and K. Bächmann, Phys. Rev. C 6, 1362 (1972).
[17]P. M. Starzyk and N. Sugarman, Phys. Rev. C 8, 1448 (1973).
[18]J. M. Miller and J. Hudis, Annu. Rev. Nucl. Sci. 9, 159 (1959).
[19]E. K. Hyde, *The Nuclear Properties of the Heavy Elements* (Prentice-Hall, Englewood Cliffs, New Jersey, 1964), Vol. III.
[20]J. Hudis, in *Nuclear Chemistry*, edited by L. Yaffe (Academic, New York, 1968), Chap. 3; J. Hudis, Phys. Rev. 171, 1301 (1968).
[21]J. Gindler and J. R. Huizenga, in *Nuclear Chemistry*, edited by L. Yaffe (Academic, New York, 1968), Vol. II, p. 1.
[22]N. T. Porile, Phys. Rev. 141, 1082 (1966).
[23]E. Hagebø, J. Inorg. Nucl. Chem. 32, 2489 (1970).
[24]J. A. Panontin and N. T. Porile, J. Inorg. Nucl. Chem. 33, 3211 (1971).
[25]V. U. Trabitzsch and K. Bächmann, Radiochim. Acta 16, 15 (1971).
[26]V. U. Trabitzsch and K. Bäckmann, Radiochim. Acta 16, 129 (1971).
[27]J. R. Nix and W. J. Swiatecki, Nucl. Phys. 71, 1 (1965).
[28]J. R. Nix, Ann. Phys. (N.Y.) 41, 52 (1967).
[29]J. B. Cumming, Annu. Rev. Nucl. Sci. 13, 261 (1963).
[30]G. W. Leddicotte, *The Radiochemistry of Rubidium* (U.S. Atomic Energy Commission, Washington, D. C., 1962).
[31]C. M. Lederer, J. M. Hollander, and I. Perlman, *Table of Isotopes* (Wiley, New York, 1967), 6th edition.
[32]J. B. Cumming, *Application of Computers to Nuclear and Radiochemistry* (U.S. Atomic Energy Commission, Washington, D.C., 1962).
[33]J. H. Davies and L. Yaffe, Can. J. Phys. 41, 762 (1963).
[34]Y. Y. Chu, University of California Radiation Laboratory Report No. UCRL-8926, 1959 (unpublished).
[35]J. A. Panontin and N. Sugarman, J. Inorg. Nucl. Chem. 25, 1321 (1963).
[36]L. C. Northcliffe and R. F. Schilling, Nucl. Data A7, 233 (1970).
[37]N. Bohr, K. Dan. Vidensk. Selsk. Mat.-Fys. Medd. 18, No. 8 (1948).
[38]J. Lindhard, M. Scharff, and H. E. Schiøtt, K. Dan. Vidensk. Selsk. Mat.-Fys. Medd. 33, No. 14 (1963).
[39]N. K. Aras, M. P. Menon, and G. E. Gordon, Nucl. Phys. 69, 337 (1965).
[40]C. D. Moak and M. D. Brown, Phys. Rev. 149, 244 (1966).
[41]M. Pickering and J. M. Alexander, Phys. Rev. C 6, 332 (1972); 6, 343 (1972).
[42]J. C. D. Milton and J. S. Fraser, Can. J. Phys. 40, 1626 (1962).
[43]J. M. Alexander and M. F. Gazdik, Phys. Rev. 120, 874 (1960).
[44]P. Kruger and N. Sugarman, Phys. Rev. 99, 1459 (1955).
[45]E. M. Franz and G. Friedlander, Phys. Rev. C 4, 1671 (1971).
[46]J. B. Cumming, P. E. Haustein, R. W. Stoenner, L. Mausner, and R. A. Naumann, Phys. Rev. C 10, 739 (1974).
[47]V. P. Crespo, J. B. Cumming, and J. M. Alexander, Phys. Rev. C 2, 1777 (1970).
[48]N. Metropolis, R. Bivins, M. Storm, A. Turkevich, J. M. Miller, and G. Friedlander, Phys. Rev. 110, 185 (1958); N. Metropolis, R. Bivins, M. Storm, A. Turkevich, J. M. Miller, and G. Friedlander, Phys. Rev. 110, 204 (1958).
[49]I. Distrovsky, P. Rabinowitz, and R. Bivins, Phys. Rev. 111, 1659 (1958).
[50]W. D. Myers and W. J. Swiatecki, Nucl. Phys. 81, 1 (1966); Y. Yamaguchi, Prog. Theor. Phys. 6, 529 (1951).
[51]G. Rudstam, E. Bruninx, and A. C. Pappas, Phys. Rev. 126, 1852 (1962).
[52]K. Chen, Z. Fraenkel, G. Friedlander, J. R. Grover, J. M. Miller, and Y. Shimamoto, Phys. Rev. 166, 949 (1968).
[53]H. W. Bertini, Phys. Rev. C 6, 631 (1972).
[54]R. Brandt, F. Carbonara, E. Cieslak, M. Dakowski, C. Gfeller, H. Piekarz, J. Pierkarz, W. Riezler, R. Rinzivillo, E. Sassi, M. Sowinski, and J. Zakrzewski, Nucl. Phys. A90, 176 (1967).
[55]J. B. Cumming, R. W. Stoenner, and P. E. Haustein, Phys. Rev. C 14, 1554 (1976).
[56]J. Gosset, H. H. Gutbrod, W. G. Meyer, A. M. Poskanzer, A. Sandoval, R. Stock, and G. D. Westfall, Phys. Rev. C 16, 629 (1977).
[57]G. D. Westfall, J. Gosset, P. J. Johansen, A. M. Poskanzer, W. G. Meyer, H. H. Gutbrod, A. Sandoval, and R. Stock, Phys. Rev. Lett. 37, 1202 (1976).
[58]R. Serber, Phys. Rev. 72, 1008 (1947); 72, 1114 (1947)
[59]N. Sugarman, M. Campos, and K. Wielgoz, Phys. Rev. 101, 388 (1956).
[60]N. T. Porile and N. Sugarman, Phys. Rev. 107, 1410 (1957).
[61]N. Sugarman, H. Münzel, J. A. Panontin, K. Wielgoz, M. V. Ramaniah, G. Lange, and E. Lopez-Menchero, Phys. Rev. 143, 952 (1966).
[62]M. Lagarde-Simonoff, S. Regnier, H. Sauvageon, and G. N. Simonoff, Nucl. Phys. A250, 369 (1976).
[63]M. Lagarde-Simonoff, Internal Report CENBG, 1974 (unpublished).
[64]E. Hagebø and T. Lund, J. Inorg. Nucl. Chem. 37, 1569 (1975).